MS.ID-IJPBS-2187
International Journal of Pharmacy and Biological Sciences-IJPBS™ (2023) 13 (4): 28-35
Online ISSN: 2230-7605, Print ISSN: 2321-3272
Research Article | Biological Sciences | OA Journal | MCI Approved | Index Copernicus

Estimation of Variation Dose in Pediatric Phantom Study Using Digital Radiography

Gokulchandra Singh Oinam[1,2,3,4], Majed Naif Allharbi[1,2,3,4], Naif Abdulrahim Alanazi[1, 2, 3, 4], Faisal Awadh Alanazi[1,2, 3, 4], Fayaz Ul Haq[1, 2, 3, 4] and Abdullah Al Shahrani [3,4,5]

[1]Radiological Sciences Program, College of Applied Medical Sciences, Riyadh, Saudi Arabia,
[2]King Saud Bin Abdul-Aziz University for Health Sciences, Riyadh Saudi Arabia,
[3]King Abdullah, International Medical Research Centre (KAIMRC), Riyadh, Saudi Arabia,
[4] King Abdul-Aziz Medical City, Ministry of National Guard - Health Affairs, Riyadh, Saudi Arabia.
[5]Medical Imaging Department, King Abdul-Aziz Medical City, Ministry of National Guard-Health Affairs, Riyadh, Saudi Arabia.

Received: 02 Jul 2023/ Accepted: 9 Aug 2023 / Published online: 1 Oct 2023
***Corresponding Author Email:** oinamg@ksau-hs.edu.sa

Abstract

Aim: The aim of this study was to reduce radiation dose with the pediatric phantom by modifying the exposure and filtering parameters without reducing the image quality. **Materials & Methods:** The images were acquired using a Pediatric Anthropomorphic Training Phantoms CIRS Model 715 Series and a digital X-ray detector. The phantom was placed in a supine position in all views such as hand (Anterior-Posterior, oblique) and ankle (Anterior-Posterior, Oblique). Different mAs values were used to create three dosage protocols (high, medium and low); each technique also included copper (Cu) filtering. The ESD (Estimated Skin Dose) for each exposure was calculated using DAP (Dose Area Product). For the physical measurement of picture quality, CNR (Contrast to Noise Ratio) was computed using image. Evaluated by 15 observers the Image quality using visual grading analysis (VGA). **Results:** By using the different dosage regimen, the estimated doses were obtained, for the hand, it ranged from 4.7-45.5uGy and for the ankle it was from 52.9uGy. ESD was shown to decrease as Cu filtering was increased. There was a 0.1 in VGA score difference between high and low dosage procedures without filtering, but a 0.3 difference when filtration was used. VGA scores grew as mAs climbed. Cu filtration and projection adjustments had little effect on fracture visibility. **Conclusion:** Changing the exposure parameters in digital radiography can lower the dosage while maintaining image resolution in fractures. Without Cu filtration, excellent image quality can be attained with DP (Dorsopalmar) and oblique hand projection. Cu filtering for ankle projections, on the other hand, has little or no effect on overall image quality.

Keywords
Phantom, Dose measurement, Ankle X-ray, Hand X-ray.

*****

INTRODUCTION

Phantom studies facilitate the use of radiation dose monitoring based on descriptive radiological parameters to minimize patient doses. Digital systems were quickly replaced by analog screen film systems in the diagnostic radiology department. Despite the differences in the characteristics of the new X-ray image detectors, the same radiography protocols used for X-ray film screen applications for digital imaging systems have not yet been considered. [1] In terms of radiographic quality and radiation dose, pediatric radiography is a complex procedure. First, pediatric radiographs have significantly lower contrast. Second, it is widely recognized that radiation levels are an increasingly serious problem for pediatric patients, who are extremely sensitive to radiation. [2]

Digital radiography (DR) poses an additional challenge in matching image quality (IQ) to radiation levels. [3] The energy response from the digital square detector is basically measured. The relevant DR ratings offer great versatility when using low radiation levels and processing images that are completely different from those on film screens. [4] When radiation exposure to image detectors is underestimated compared to film screens, I.Q. Maintain or improve a diagnostically acceptable condition. [5] The best coverage is achieved using nurse victimization assistant with a Thermion valve potential near 50 kV and strong X-ray filtration to detect low to moderate contrast iodine data. [6] The best tube potential corresponds to 60 kV for low or medium-contrast metal elements and 80 100 kV for high-contrast details. [7] The low potential spectrum requires a high tube load, which may be acceptable for medical radiological examinations. An inexpensive alternative to filtration is to use an optional 25 mm zero-diameter Cu filter or an acceptable K-edge filter. [8]

Changes in beam quality can directly affect both image contrast and image sharpness. When establishing adequate metrics for evaluating image quality, both contrast and sharpness must be considered. [9] Pediatric patients are more susceptible to the harmful effects of ionizing radiation than adults because of their faster cell division and longer life expectancy. Due to the lack of natural contrast in pediatric limb imaging, imaging parameters must improve to keep patient exposure "as low as reasonably achievable" (ALARA). Optimization can also reduce the risk to pediatric patients by reducing the radiation dose by minimizing the number of retake requests. [10]

Study Phantom

Pediatric Anthropomorphic Training Phantoms CIRS Model 715 Series shown in Figure 1& 2. Fractures were discovered on the left side of the phantom (13) (14). The hand and the ankle were chosen as the study's two locations. Children's hand fractures are among the most common, although ankle fractures are frequently misdiagnosed.

Figure 1: Pediatric Phantoms Model Series CIRS 715

Figure 2: Oblique ankle & left oblique hand.

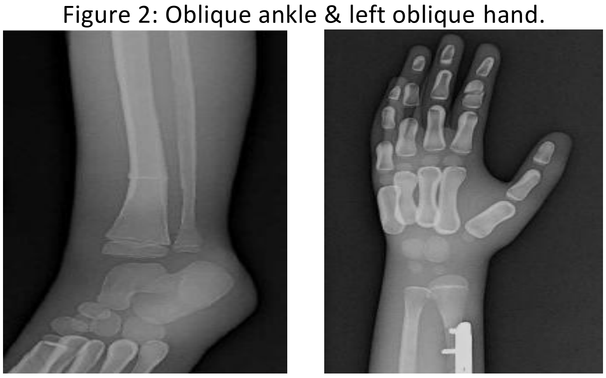

Imaging Systems and Positioning

All the images were taken with Arcoma X-ray imaging equipment with DAP integration. Cu filtering of 0.1, 0.2, or 0.3 mm can be installed in the X-ray tube (16). The photographs were all captured with a Canon DR (CXDI701C Wireless Universal) indirect detector with a cesium iodide scintillator with a detective quantum efficiency (DQE) of more than 70%. With a 35x43cm effective imaging area, this detector has 125x125m pixels and a 2800x3408 pixel image matrix. With 4096 gradations, the detector's resolution is 4.0lp/mm (17). (18). No anti-scatter grid was used in this study since it would increase the patient dosage (19). In the supine position, the phantom was scanned for both anterior-posterior (AP) and oblique projections pertinent to hand and ankle x-ray. For the oblique projection, a radiolucent pad was placed beneath the phantom, which was positioned at 20 degrees obliquity. The collimated field stayed constant at 15x26cm with a source-to-image distance (SID) of 110 cm. With a collimated field of 14.5x8cm and a SID of 110cm, dorsopalmar (DP) and lateral standard hand projections were also produced (20). The focal point of both hand projections is modest, but the focal point of both ankle projections is enormous.

Protocol

Ankle and Hand X-ray

Thirty-six exposures were taken, with six for each projection. Three different imaging dosage regimens were used: low, medium, and high. Standard exposure settings were used in the high-dosage experiment, the tube potentials for the DP and Oblique hand projections were 52 kVp and 56 kVp, respectively. A tube intensity time product of 1mAs and 1.6mAs were used for DP and Oblique hand projections. For the AP ankle projection, a voltage of 55 kVp and a current of 1.6 mAs was employed, while for the oblique ankle projection, a voltage of 57 kVp and 1.63 mAs was used. For each projection, the exposure factor was created three phases, and low, medium and large protocols (Tables 1 and 2). Cu filtration was tested using no filtration as well as 0.1 mm and 0.2 mm extra Cu filtration for each protocol (Table 1.)

Dose Measurement

A calibrated integrated ionization chamber was used to get dose area product (DAP) values. The entrance skin dose (ESD) for each exposure was calculated using DAP. The collimated field size is represented by A, and the backscattering coefficient is denoted by BSF using the below equation. For this study, Toivonen et al. proposed a backscatter coefficient of 1.3. (21).

ESD = DAB/A * BSF (eq.1)

Where 'A' is the size of the collimated x-y beam and 'BSF' the backscattered factor.

Image quality

The contrast-to-noise ratio (CNR) is a physical measure of image quality that has been used to characterize it. The influence of variations in beam quality on image quality is assessed using CNR. (22) Images are used to establish CNR calculations' areas of interest (ROIs). The standard deviation of the bone is represented as **'a_1'**. In each of the 36 total photos, four ROIs were put on a uniform area, two on soft tissue and two on bone.

(Figure 2) for the two ROIs placed on soft tissue and the two placed on bone, a mean value was calculated to obtain measurements that were more reliable using equation 2.

CNR= $(S_1 - S_2)/a_1$ (Eq.2)

Twelve observers were assessed the image using visual image quality grading analysis consisting of ten diagnostic radiography students (years 3-4) and two well experienced radiographers. The latest version of View DEX (Viewer for Digital Evaluation of X-ray Images) was used to display the image consisting of visual scoring criteria and collected observer scores. For better reliability and validity, the observer was properly trained in visual assessment ahead of image- viewing. Few criteria to the observer were notified to the observer such as windowing was prohibited but pan and zoom were allowed to use. The observers first scored the chest images followed by wrist and leg. All images, exposure factor information and acquisition condition were randomized and blinded. A five- point Likert scale scoring criteria was used to assess five criteria: Overall image quality, contrast, sharpness, and noise and fracture visibility. Within the scale, a score of 1 indicate Poor, and 5 indicates Excellent. All observer information was anonymized. To facilitate this study, numerical scales were used to simplify information and consistent observer agreement ((Svensson, 2010). Viewing condition of observation room such as ambient lighting conditions should remain constant throughout the image- viewing process less than 10 lux (Park,2008: Brennan,2007). A monitor with an area of 30.6 x 40.8 cm was used for observer analysis. Images were displayed on a 2 Megapixel, 20.1-inch monochrome LCD ME201L/r with DICOM calibrated enables grayscale presentation. Calculation was made using VGA (VGA_T) equation 3:

$VGA_T = (\#_{O,I}\, S_C) / N_i\, N_o$(Eq. 3)

Where S_C is the criterion score given by observers, O is the observer, and I is the image. Ni is the total number of the image and N_o is the total number of observers. VGA_{CSN} was calculated from the observer scores for three image quality parameters such as contrast, sharpness, and noise. Moreover, the VGA_{CSN} was correlated with the fracture visibility for each radiographic projection.

Statistics:

Descriptive statistics were used to analyze the data. The collected data was entered into Microsoft Excel and transferred to SPSS version 23 for statistical analysis. The findings are presented with mean VGA, CNR and R2 correlation as illustrated in table below**.** A nonparametric Kruskal-Wallis test was used to analyze the significant difference at 95% confidence interval between the 12 observers regarding the VGA.

Table 1: Image Acquisition Protocol

Dose level	Anatomic view	Incidences	kV	mAs	Cu Filter
low	Hand	Dorso-palmar	52	1	none
					0.1mm
					0.2mm
		Oblique	56	1.6	none
					0.1mm
					0.2mm
	Ankle	AP	56	2	none
					0.1mm
					0.2mm
		Oblique	55	1.6	none
					0.1mm
					0.2mm
medium	Hand	Dorso-palmar	52	1	none
					0.1mm
					0.2mm
		Oblique	56	1.6	none
					0.1mm
					0.2mm
	Ankle	AP	56	2	none
					0.1mm
					0.2mm
		Oblique	55	1.6	none
					0.1mm
					0.2mm
large	Hand	Dorso-palmar	52	1	none
					0.1mm
					0.2mm
		Oblique	56	1.6	none
					0.1mm
					0.2mm
	Ankle	AP	56	2	none
					0.1mm
					0.2mm
		Oblique	55	1.6	none
					0.1mm
					0.2mm

RESULTS:

Dose & Contrast-to-Noise Ratio measurements.

In Table 2: presents the ESD and DAP for all of the following small, medium and last large dose protocols for the hand. The ESD for the small was from 4.7-40.8, for medium 5.2-44.5 and the large from 4.7-45.5. The overall ESD measurements were from 4.7-45.5. Moreover, the average of the ESD is 4.13. The DAP for the small was from 0.047-0.434, for medium 0.048-0.433 and the large from 0.047-0.436. And for the DAP the measurements average were from 0.047-0.436, and the average was 0.118.

Table 2: Dose & Contrast-to-Noise Ratio measurements for Hand

ESD	VGA$_T$	DAP	CNR	Cu filter (mm)	mAs	Kvp	Projection	Hand
24 uGy	4.1	0.235 mGy / 0.533 dGy cm2	38.8%	0M	1	52	AP	Small
9.5 uGy	3.5	0.091 mGy / 0.136 dGy cm2	25.3%	0.1	1	52		
4.7 uGy	2.7	0.047 mGy / 0.070 dGy cm2	18.6%	0.2	1	52		
40.8 uGy	3.8	0.434 mGy / 0.608 dGy cm2	33.9%	0	1.6	56	Oblique	
17.6 uGy	2.8	0.186 mGy / 0.261 dGy cm2	23.6%	0.1	1.6	56		
9.5 uGy	2.1	0.099 mGy / 0.139 dGy cm2	21.4%	0.2	1.6	56		
27.2 uGy	3.3	0234 mGy / 0.674 dGy cm2	36.6%	0	1	52	AP	Medium
10.3 uGy	2.8	0.092 mGy / 0.205 dGy cm2	25.6%	0.1	1	52		
5.2 uGy	1.8	0.048 mGy / 0.106 dGy cm2	20.9%	0.2	1	52		
44.5 uGy	4.5	0.433 mGy / 0.576 dGy cm2	36.5%	0	1.6	56	Oblique	
18.8 uGy	3.9	0.181 mGy / 0.241 dGy cm2	32.7%	0.1	1.6	56		
9.3 uGy	4.1	0.102 mGy / 0.135 dGy cm2	30.1%	0.2	1.6	56		
24 uGy	4.1	0.228mGy / 0.378 dGy cm2	35.4%	0	1	52	AP	Large
9.5 uGy	3.8	0.091 mGy / 0.151 dGy cm2	29.4%	0.1	1	52		
4.7 uGy	3.5	0.047 mGy / 0.078 dGy cm2	26.9%	0.2	1	52		
45.5 uGy	4.3	0.436 mGy / 0.637 dGy cm2	39.2%	0	1.6	56	Oblique	
19 uGy	3.9	0.186 mGy / 0.272 dGy cm2	33.5%	0.1	1.6	56		
10.3 uGy	3.2	0.102 mGy / 0.149 dGy cm2	32.8%	0.2	1.6	56		

In Table 3, demonstrates the ESD and DAP for the small, medium, and large dose protocols for ankle. The ESD for the small was from 10.3-52.6, for medium 10.8-52.9 and the large from 10.9-52.8. The overall of ESD the measurements were from 10.3-52.9. Moreover, the average of the ESD was 0.815. The DAP for the small was from 0.098-0.477, for medium 0.098-0.477 and the large from 0.101-0.476. And for the DAP the average measurements were from 0.098-0.477, and the average is 0.762.

Demonstrates the CNR for the small, medium, and large for hand and ankle in dose protocols. Beginning with hand in CNR, for the small was from 18.6-38.8, for medium 20.9-36.6 and the large from 26.9-39.2. Similarly for the ankle, for the small was from 14.8-23.1, for medium 14.1-22.2 and the large from 13.4-22.9. The overall of CNR the measurements the hand was from 18.6-39.2, and the average is 0.59. Moreover, the overall of CNR the measurements for the ankle were from 13.4-23.1, and the average is 0.815. The protocol for hand, and ankle with dose measurements and image quality are represented in Table (1). As illustrated in Table (1), (2) and (3), dose measurement and CNR are decreased with increase filtration thickness. The most substantial reduction in CNR and dose measurement is found with 0.2 filter Cu. To conclude our study, it’s clearly demonstrated that an increase in filtration will reduce patient doses and overall reduction in image quality

Table 3: Dose & Contrast-to-Noise Ratio measurements for Ankle

ESD	VGAT	DAP	CNR	Cu filter (mm)	mAs	Kvp	Projection	Ankle
48.8 uGy	3.1	0.433mGy / 0.855 dGy cm2	23.1%	0	2	55	AP	Small
20.2 uGy	2.8	0.183mGy / 0.861 dGy cm2	17.4%	0.1	2	55		
10.3 uGy	2.4	0.098 mGy/ 0.194 dGy cm2	14.8%	0.2	2	55		
52.6 uGy	3.8	0.477 mGy / 1.302 dGy cm2	17.9%	0	1.6	56	Oblique	
22.5 uGy	3.6	0.207 mGy / 0.555 dGy cm2	15.9%	0.1	1.6	56		
12 uGy	3	0.115 mGy / 0.314 dGy cm2	15.5%	0.2	1.6	56		
48.6 uGy	3.5	0.432 mGy / 0.854 dGy cm2	22.2%	0	2	55	AP	Medium

20.4 uGy	2.9	0.183 mGy / 0.362 dGy cm2	18.7%	0.1	2	55		
10.8 uGy	2.7	0.098 mGy / 0.194 dGy cm2	14.1%	0.2	2	55		
52.9 uGy	3.4	0.477 mGy / 1.397 dGy cm2	18.4%	0	1.6	56		
22.6 uGy	3	0.209 mGy/ 0.610 dGy cm2	16.7%	0.1	1.6	56	Oblique	
12.2 uGy	2.8	0.115mGy/ 0.336 dGy cm2	14.2%	0.2	1.6	56		
48.6 uGy	3.7	0.440 mGy / 1.449 dGy cm2	22.6%	0	2	55		
20.7 uGy	2.8	0.186 mGy / 0.611 dGy cm2	18.9%	0.1	2	55	AP	
10.9 uGy	2.8	0.101 mGy / 0.332 dGy cm2	17.1%	0.2	2	55		Large
52.8 uGy	3.7	0.476 mGy / 1.170 dGy cm2	22.9%	0	1.6	56		
22.6 uGy	3.5	0.207 mGy / 0.509 dGy cm2	16.2%	0.1	1.6	56	Oblique	
12.1 uGy	3.8	0.115 mGy / 0.262 dGy cm2	13.4%	0.2	1.6	56		

Visual and Physical Image Quality Measurements

In Table 4, it is noted that for each of the four projections, the fracture visibility was correlated with the contrast-to-noise ratio (CNR) and visual measurement (VGA_{CSN}). There was a strong correlation between CNR and fracture visibility for both AP and oblique hand views. Further for the AP ankle there was a strong correlation between the CNR and fracture visibility as well. In regard to oblique ankle projection, a moderate correlation was found between the CNR and fracture visibility. Similar findings can also be seen between the VGA_{CSN} and fracture visibility with strong correlation noted in wrist AP, lateral hand, and ankle AP projection. The weakest correlation was found in the oblique ankle projection.

The mean score for the observer shows no statistical difference in VGA_T score between the observers. A strong correlation was found between the physical measurement of CNR and visual analysis of each image. However, oblique ankle projection reported to be weakest correlation than other projections.

Table 4: R2 correlation coefficients between CNR, VGACSN and fracture visibility

Projection	CNR vs Fracture Visibility	VGA_{CSN} vs fracture visibility
Hand AP	0.8645	0.9865
Oblique Hand	0.6321	0.6551
AP ankle	0.6535	0.7452
Oblique ankle	0.4358	0.5655

DISCUSSION:

The goal of this study is to minimize radiation dosage without compromising picture quality by employing pediatric phantoms with several bones of interest, such as the hand and ankle. Variations in exposure parameters and beam filter settings are included. This study's low-dose photos revealed that dose reduction resulted in negligible density.

CNR values, on the other hand, differ dramatically among dosage procedures and anatomical areas. Other research has yielded similar results. (11) The CNR values recorded for the ankle are much lower than those reported for the hand projection. Observers who reported difficulty reflected this large decline in comments. However, phantom placement and overlapping anatomy, particularly in the oblique view, may be contributing to these issues. The findings of this investigation reveal that visual and physical measurements in each projection have a good association, validating our findings. This strong link raises the following question: is it necessary to examine image quality using both physical and visual measurements? Similarly, Overall image quality scores are similar, implying that overall image quality alone may not be enough to forecast this. Other research has shown similar findings. (10) A low standard deviation for inter-observer scores indicates that observers agree on each criterion. The effect of Cu filtration on dose and picture quality was the most dramatic finding of this investigation, with further filtering continuing to lower patient doses at the expense of image quality. The ESD and DAP values observed in this investigation are consistent with those found in previous research. (12)-(13). Physical measurements were taken for each of the 54 photographs using CNR, a widely used method of determining image quality, and visual measurements were taken when the images were reviewed by eight observers.

Pediatric Phantom Dose Optimization Using Digital Radiography with Variation of Exposure Parameters and Filtration while minimizing Image Quality Impairment

This study has similarity to our study concept which is reducing dose without losing image quality. Also, did the same wrist and rib projections using Cu filtration.

The study aimed to reduce radiation dose without compromising image quality, Variation of exposure parameters and beam filtration settings were involved. A reduced dose has little effect on fracture visibility, according to the low-dose images created in this study. The CNR values, on the other hand, differ significantly between dose protocols and anatomical regions. Other research has achieved similar results. The CNR values for ankle projections are significantly lower than for hand projections. Observers commented on how difficult it was to visualize fractures, indicating that this was a significant drawback. However, phantom positioning and the superimposition of anatomical structures, especially in the oblique view, could be contributing to the difficulty.

Variation of exposure parameters in digital radiography can achieve a dose reduction without compromising diagnostic image quality or fracture visibility. Without the use of Cu filtration, superior image quality can be achieved for AP and lateral hand projections at higher doses. Cu filtration for ankle projections, on the other hand, can reduce phantom dose while having almost no effect on overall image quality. The addition of filtration reduced doses across the board for all projections.

CONCLUSION

This study shows a strong correlation between the visual and physical measurement for each of the radiographic projections.

Financial support and sponsorship

Nil

Conflicts of interest

There are no conflicts of interest.

REFERENCES:

1. Mohammed Ali A, Hogg P, England A. Dose optimization in pediatric radiography – Using regression models to investigate the relative impact of acquisition factors on image quality and radiation dose. Physica Medica. 2019 Dec; 68:61–8.
2. Tapiovaara MJ, Sandborg M, Dance DR. A search for improved technique factors in paediatric fluoroscopy. Physics in Medicine and Biology. 1999 Jan 1; 44(2):537–59.
3. Jones A, Ansell C, Jerrom C, Honey ID. Optimization of image quality and patient dose in radiographs of pediatric extremities using direct digital radiography. The British Journal of Radiology. 2015 Jun; 88(1050):20140660.
4. Shahgeldi K, Sjöberg T, Nordström J, Lesanu R, Svahn TM. Optimizing image quality, radiation dosage to the patient and to the detector in pediatric chest radiography: A phantom study of a portable digital radiography system. Radiation Protection Dosimetry. 2019. doi:10.1093/rpd/ncz028
5. Moey, S., Shazli, Z. A Phantom Study for the Optimization of Image Quality and Radiation Dose for Common Radiographic Examinations in Digital Radiography. Iranian Journal of Medical Physics, 2018; 15(4): 271-276. doi: 10.22038/ijmp.2018.29825.1325
6. Bond N. Optimization of image quality and patient exposure in chest radiography. Radiography. 1999 Feb;5(1):29–31
7. Precht H, Gerke O, Rosendahl K, Tingberg A, Waaler D. Digital radiography: optimization of image quality and dose using multi-frequency software. Pediatric Radiology. 2012 Apr 17; 42(9):1112–8.
8. Davis AT, Safi H, Maddison SM. The reduction of dose in paediatric panoramic radiography: the impact of collimator height and programme selection. Dentomaxillofacial Radiology. 2015 Feb; 44(2):20140223.
9. Jamal NHM, Sayed IS, Syed WS. Estimation of organ absorbed dose in pediatric chest X-ray examination: A phantom study. Radiation Physics and Chemistry. 2020; 166:108472. doi: 10.1016/j.radphyschem.2019.108472
10. Jones A, Ansell C, Jerrom C, Honey ID. Optimization of image quality and patient dose in radiographs of paediatric extremities using direct digital radiography. The British Journal of Radiology. 2015 Jun; 88(1050):20140660
11. Knight SP. A paediatric X-ray exposure chart. J Med Radiat Sci. 2014; 61(3):191–201.
12. Toivonen M. Patient dosimetry protocols in digital and interventional radiology. Radiat Prot Dosim. 2001; 94(1–2):105–8.
13. Burger W, Burge M. Digital Image Processing: An Algorithmic Introduction Using Javae. 2008. p. 2.

14. Mori M, Imai K, Ikeda M, Iida Y, Ito F, Yoneda K, et al. Method of measuring contrast-to-noise ratio (CNR) in nonuniform image area in digital radiography. Electron Commun Japan. 2013; 96(7):32–41.
15. Svensson S, Zachrisson S, Svalkvist A, Ba M, Ha M, Radiology D, et al. View Dex: an Efficient and Easy-To- Use Softw Are. Radiat Prot Dosimetry. 2010; 139(1):42–51.
16. Park CM, Lee HJ, Goo JM, Han DH, Kim JH, Lim KY, et al. Comparison of observer performance on soft-copy reading of digital chest radiographs: High resolution liquid-crystal display monitors versus cathode-ray tube monitors. Eur J Radiol. 2008; 66(1):13– 8.
17. Brennan PC, McEntee M, Evanoff M, Phillips P, O'Connor WT, Manning DJ. Ambient lighting: effect of illumination on soft copy viewing of radiographs of the wrist. AJR Am J Roentgenol. 2007; 188(2):177–80.
18. Tashiro T, Manager G. 510 (k) summary; Monochrome LCD monitor MS25i2 (ML21025. 2013; 10:8.
19. McGinty, G, Allen B, Wald C. Imaging 3.0 ACR IT Reference Guide for the Practicing Radiologist. Am Coll Radiol. 2013; 1–11.
20. Mansson LG. Methods for the Evaluation of Image Quality: A Review. Radiat Prot Dosimetry. 2000; 90(1):89– 99.
21. Lanca, Luis; Silva A. Digital Imaging Systems for Plain Radiography. Lisbon: Springer; 2013. P.173.
22. Mukaka MM. A guide to appropriate use of Correlation coefficient in medical research. Malawi Med J. 2012; 24(3):69–71.
23. Rennie L, Court-Brown CM, Mok JYQ, Beattie TF. The epidemiology of fractures in children. Injury. 2007; 38(8):913–22.
24. Svensson S, Zachrisson S, Svalkvist A, Ba M, Ha M, Radiology D, and et al. View Dex #: an Efficient and Easy-To-Use Softw Are. Radiat Prot Dosimetry. 2010;139(1):42-51
25. Park CM, Lee HJ, Goo JM, Han DH, Kim JH, Lim KY, et al. Comparison of observer performance on soft copy reading of digital chest radiographs: High resolution liquidcrystal display monitors versus cathode-ray tube monitors. Eur J Radiol. 2008; 66(1):13-8.
26. Brennan PC, McEntee M, Evanoff M, Phillips P, O'Connor WT, Manning DJ. Ambient lighting: effect of illumination on soft copy viewing of radiographs of the wrist. AJR Am J Roentgenol. 2007;188(2):177-80
27. Lança, Luis & Bowdler, Matthew & Creedon, Jill & Dayer, Valentin & Stensholt, N & Stuivenberg, Vera & Pinhao, S & Visser, M & Pires, J. (2018). Paediatric phantom dose study using digital radiography with variation of exposure parameters and filtration.